PRACTICAL FORMULAS OF THE CURVED BRIDGE WITH MULTIPLE PLATE GIRDER

(Trans. of JSCE, No.93 May, 1963, pp. 1~9)

By Dr. Eng., Sadao Komatsu C.E. Member

1. Introduction

The practical formulas for design work of the curved bridge with multiple plate girders spaced along the concentrical circles is derived. In previous papers, authors developed the fundamental theory of most general curved girder bridge and found its explicit solutions by the three dimensional analysis. Applying the results, we can rationally calculate about this kind of bridge structure through the following process;

(a) taking in account of the radius of curvature, we firstly calculate the important fundamental quantities concerned with the transverse section of bridge,

(b) and then calculate both stress resultants and distorsions in the whole section of bridge by the analysis in three dimensions based on the assumption that the transverse section of bridge does not deform at all,

(c) finally determine the maximum stress as well as the reactions from the stress resultants by using described formulas that contain influence of the curvature.

The process (a) shall be given at section 3 ~ 6.

2. Loading condition in the case of torsion bending

In the case where the resultants of external load pass through the center of curvature 0, the torsion bending will be able to occur without symmetrical bending.

3. Centroid of transverse section of curved bridge. (Fig. 2)

The rectangular coordinates $(\bar{y}_0, \bar{z}_0)$ to determine the situation of centroid are given by formula (10), where F_{sj} is the cross sectional area, R_j is the radius of curvature, and (y_j^*, z_j^*) are rectangular coordinates of a centroid of the j th girder.

Furthermore $\sum_j'$ denotes the summation over the transverse section of bridge.

4. Flexural properties of the transverse section of bridge. (Fig. 3)

The moment of inertia asout $0_n y$, $0_n z$ and the product of inertia with reference to these axes are given by formulas (12), where $I_{\bar{y}j}$, $I_{\bar{z}j}$ and $I_{\bar{y}\bar{z}j}$ are the moments of inertia and the product of inertia about $0_j\bar{y}_j$, $0_j\bar{z}_j$ at the section of the j th girder alone, 0_n, 0_j are the centroids of the transverse section of bridge and the j th girder respectively, (y_{oj}, z_{oj}) are (y, z) coordinates of centroid 0_j, and finally (y, z) are rectangular coordinates taken in the horizontal and virtical directions through an origin 0_n.

5. Shear center in transverse section of bridge

Denoting the z coordinate of shear center S in the transverse section of bridge by z_s, and that of the j th girder alone by z_j, we can determine the situation of the shear center S by formulas (22) as well as (24)', where R_o is distance between shear center S and the center of curvature 0 and R_{oj} is that of shear center S_j concerned with the j th girder alone.

In most general bridge, we may take R_{oj} to be equal to R_j.

6. Torsional resistance and torsion bending constant

The torsional resistance J as well as the torsion bending constant C_w of the transverse section of bridge are given by formulas (31) and (32) respectively.

7. Distributed shear forces in each main girder

Under arbitrary virtical loading, the cross girder in cooperation with the lateral bracing have important action in distributing the load to each main girders. Due to this phenomena, the shear force Q_j induced in the cross section of the j th girder is given as a function of four stress resultants i.e. total shear force Q, total torsional moment T, St. Venant's torsional moment Ts and secondary torsional moment T_W by formula (34), where J_j, C_{wj} represent torsional resistance and torsion bending constant of the j th girder respectively, and $Y_j = R_{oj} - R_o$.

8. Distributed torsional moments in each main girder

The torque T_j developed by each girder is obtained by formula (36).

9. Distributed bending moments in each main girder

The bending moment $M_{\bar{y}_j}$ induced in the j th girder is given by formula (37), where $d^2\theta/d\varphi^2+\theta$ is nothing but distorsions and some solutions for them are shown as the function of situation of transverse section in Table-1 corresponding to various loading conditions.

10. Reactions at supports

(1) I-girder bridge (Fig. 5a)

A reaction R_{ja} at the support $\varphi = a$ under the web plate in the j th girder is girder is readily obtained as the difference between two shear forces $Q_{j,\varphi=a\ -\ 0}$ at just front section and $Q_{j,\varphi=a\ +\ 0}$ at just behind section of the support. The relation among them is seen in formula (38)

(2) Box girder bridge (Fig. 5b)

In the case of a box girder, two supports are generally placed on a pier to resist to torsion, since we need to find the reactions at each supports. So both outside reaction R_{ja} and the inside reaction R_{ji} are readily obtained in formulas $(39)_1$ and $(39)_2$ respectively.

11. Torsional function

If the j th girder has one cellular section, and its breadth is considerably small comparison with the radius of curvature, the torsional function q_j may be given by formula (40) approximately.

12. Stress formulas

(1) Normal stress

The normal stress σ_j at any point in cross section of the j th girder is easily obtained by well-known formula (41).

(2) Shear stress

The shear stress τ_j at any point in cross section of the j th girder is also obtained by formula (42). In this formula the 1st term is shear stress due to bending and the 2nd one is due to St. Venant's torsion.

13. Secondary stress in I-girder bridge

Under arbitrary virtical loading the tension or compression along the axis of flange plate always applies. Due to resultant of them in direction of the radius through a center of curvature 0, the local bending can be developed in the flange plate, therefore the secondary stress must be added to primary stress σ_j described in section 12 for evaluating the maximum stress of cross section.

Let me propose four approximate formulas (43)~(46) for the secondary stress σ_2 corresponding to the situations of the panels and the cross sections in question of the j th girder. In order to decrease the secondary stress in flange plate, it is much favorable to make us of box girder for the curved bridge.

14. Stress resultants in cross girder (Fig. 7)

The bending moment and the shear force at the middle section of cross girder situated between the j th main girder and the j + 1 th one are gradually found by solving a pair of formulas (47) and (48) in the order of the magnitude of number j.

(Recieved Sept. 13, 1962)

ON THE BOND STRESS DISTRIBUTION ALONG ROUND BARS, DEFORMED BARS AND TWISTED DEFORMED BARS

(Trans. of JSCE, No.93 May, 1963, pp. 23～30)

By Dr. Eng., Takaaki Mizuno, C. E. Member
and
Akira Watanabe, C. E. Member

The authors measured the bond stress distribution along various reinforcing bars by improving the method of Mains. At first a half section of a bar was milled out and then the other half section was milled to provide a longitudinal channel to allow several electric strain gages to be mounted and the lead wires to be drawn out. Two halves with strain gages were combined together into a single specimen by means of the bonding compound, instead of tack welding by Mains. This method was effective for prevention of heating of the gages as well as for water-proof. A special enamel wire 0.35 mm in diameter was used as a lead wire.

As the bond stress is computed from the difference of normal forces acting on two adjacent sections, the former can be translated from the normal stress distribution measured by a series of strain gages.

The authors made the pull-out tests, the push-out tests, the beam bond tests, and at the same time the beam crack tests.

In the pull-out tests, a marked difference in the tendency of bond stress distribution was recognized between the round bars with the deformed bars and twisted deformed bars.

In the case of round bars, we can distinguish the following three stages. At the beginning of test, the maximum bond stress and the effective bond length increase as well, according as the load increases. At the next stage, the increase of the effective bond length is remarkable, but the increase of the stress itself is not so much. At last, the maximum bond stress increases rapidly and the failure takes place.

On the contrary, in the cases of deformed bars and twisted bars, the effective bond length is shorter than in the case of round bars and its enlargement is comparatively slow, in spite of the remarkable increase of the maximum bond stress due to the load increase. The peak point of the bond stress curve lies near the pulling end, staying almost immovable, and the tensile stress curve tends to zero asymptotically toward the unloaded end.

In the push-out tests, there are always two crests of the bond stress distribution curves. The heights of these crests grow almost proportionally to the load. But for round bars, after the beginning of slip, the crest near the pushing and goes down and the other crest continues to rise, their locations not moving. For deformed bars and twisted bars, the cracks appear from the loaded end and the failures take place immediately.

In the beam bond tests, the tensile stress of bars does not necessarily increase linear from the support to the loaded point, especially for deformed bars and twisted bars. In the region of constant moment between loads, the tensile stress in round bars shows quite uniform, but the tensile stress distributions for deformed bars and twisted bars are found to be wavy. Accordingly the bond stress curves in the last cases have several positive and negative peaks.

In the beam crack tests, it was shown that for the beams reinforced with deformed bars, the number of cracks is much more than in case of the beams with round bars, but the cracks in the former are quite narrower than in the latter. These facts make the former beams beneficial to increase the ultimate load and to prevent the various troubles caused by the wide cracks.

(Recieved Oct. 22, 1962)

ON THE PROFILE OF SEDIMENTATION UPSTREAM OF DAMS

(Trans. of JSCE, No.93 May, 1963, pp. 31～39)

By Dr. Eng., Sutesaburo Sugio, C.E. Member

1. Synopsis

When we plan to construct hydraulic structures across a river, such as dams, sluice gates, and jetties, or to make river improvement works widening the river width or changing the stream course, it is very important for engineers to know how the river bed profile will be changed after the improvement. This paper describes a theoretical approach to estimate the sedimentation profile upstream of low dams after the pools are filled up perfectly with bed load materials transported from upstream of rivers. To estimate the bed profiles in existing two rivers of which the river widths along the streams change considerably, dynamic and static equilibrium bed profile theories were applied. As a result of calculations, it was made clear that the static equilibrium bed profile theory is more preferable to such rivers than the dynamic equilibrium bed profile theory, and that the control flow discharge (dominant discharge) Q_n for the equilibrium bed profile plays an important role. Moreover, some statistical studies were made to find the correlation between Q_n and the annual peak discharge of flood flow.

2. Procedure of Calculations

Suppose an alluvial channel having rectangular cross section and gradually varied width in which the flow condition is considered gradually varied steady flow. Under the condition that the rate of sediment transport is constant along a stream, so that neither scouring nor deposition occurs at any section for a given flow discharge Q, the dynamic equilibrium bed profile is calculated, while the static equilibrium bed profile is estimated under the condition that the tractive force acting on a bed is equal to the critical tractive force at any section. Experimental formula proposed by Dr. Iwagaki is used to determine the critical shear velocity for given bed materials. For the resistance low and the bed-load formula, the experimental formulas proposed by the author are used. In case where the river width changes greatly as is seen upstream of most dams, it is convenient and practical to divide a stream into several reaches and proceed with the calculation from downstream toward upstream step by step, so as to satisfy the foregoing conditions.

3. Calculations for Model Channel

For a channel having a rectangular cross section and a plan of a spindle shape with a low dam at the downstream end, the dynamic and static equilibrium bed profiles were calculated for various discharges and bed material sizes to investigate the influence of the changes in channel width and bed materials upon the bed profile. As a result of calculations, the following may be stated:

1) The bed slope in the reach where the channel width increases toward downstream is rather gentle, and sometimes reverse slope appears.

2) In a channel of which the river width changes considerably, the influence of change in the channel width is more noticeable on the dynamic equilibrium bed profile than on the static one.

3) Large flow discharge tends to make the equilibrium bed slope gentle, and small flow discharge makes the equilibrium bed slope steep, if other conditions are the same.

4) Large size of bed materials is apt to make the slope of the equilibrium bed profile steep, if other conditions are the same.

4. Examples Applied to Existing Rivers

(I) In the case of A Dam

Because about twenty six years have elapsed since A Dam was built, the reach of 11.5 km upstream of the dam is considered to be in the equilibrium state. The dynamic equilibrium bed profile calculated for various flow discharges are noticeably in disagreement with the existing profiles of both bed and water level, especially within the reach of narrow width. Accordingly, if there exist reaches of very narrow width and very wide width in a river, it seems to be inadequate to assume that the dynamic equilibrium state along the whole reach is established for a certain flood discharge. Moreover, some calculations of the static equilibrium bed profile were made to find the flood flow discharge which gives a relatively similar bed profile to the existing one, and its discharge was found to be 500 m^3/s. Therefore, the control flow discharge Q_n for the equilibrium bed profile was estimated at 500 m^3/s in this river.

(II) In the case of B Dam

B Dam is one of the most typical debris barriers in Japan, and there exists about six million cubic meters of deposited sediment upstream of the dam now. The river shape upstream of the dam is like a spindle, and the river width upstream of the dam is about 580 m at the widest section and 110 m at the most narrow section. It was built about twenty six years ago, the reach of 2 km upstream of the dam is considered to be in the equilibrium state. The calculations were performed by the static equilibrium bed profile theory, and Q_n was estimated at 600 m^3/s.

5. Relation between Q_n and annual peak discharge of flood flow

The relation between Q_n and the probability of annual peak flow discharge for the past thirty-six years at the B Dam site was investigated. It was found that Q_n corresponds to the discharge of 93% probability of exceedance. In the same way, Q_n at the B Dam site corresponds to the discharge of 80% probability, according to the records for the past twenty-nine years. As is seen in the foregoing two examples, there exist some difference in the values of Q_n. But, generally speaking, it may be said that Q_n is a

little larger than the least value among the annual peak discharge of flood flows. Provided the evaluation of Q_n and the size distribution of bed materials along the reach are made, it may be possible to estimate the equilibrium bed profile upstream of a dam.

6. Summary

This paper describes some fundamental factors to estimate the river bed profile upstream of a dam, and especially discusses the meaning of the control flow discharge (dominant discharge) Q_n for the equilibrium bed profile. The following are concluded:

1) A practical method to estimate the equilibrium bed profile upstream of a dam was proposed.

2) It is not preferable to make use of the dynamic equilibrium bed profile theory for the flood discharge, when the change of river width along the reach is considerable as is often seen upstream of a dam.

3) In the above case, the static equilibrium bed profile theory for a certain discharge Q_n, which is named the control flow discharge, gives a relatively similar bed profile to the existing one.

4) This process of calculation by the static equilibrium bed profile theory does not include any bed load formula which is generally unreliable in accuracy, so it is considered to yield more accurate results and lead to considerable simplification of calculations in comparison with the dynamic equilibrium bed profile theory.

5) Q_n will be possible to be estimated statistically from the past flood flow records. In the two examples of the existing rivers it was found that Q_n corresponds to the discharges of 93% and 80% probabilities of exceedance for the annual peak discharge of flood flow respectively. Generally speaking, that discharge seems to be a little larger than the least value among the annual peak discharges of flood flows.

In any existing river, therefore, if Q_n is estimated from the past records and the size distribution of bed materials can also be adequately estimated after the pool of a dam has been filled up completely with bed load materials, it will be possible to evaluate the equilibrium bed profile upstream of the dam.

(Recieved Oct. 4, 1962)

電動式

CY-196型

コンクリート供試体の高速研磨仕上げ機

（高性能供試体研磨機）　特許品

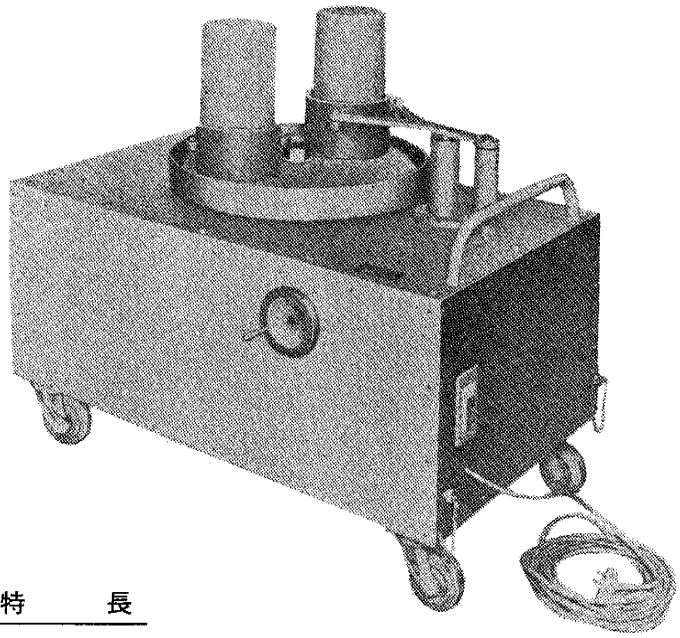

本機は試験工程および設備革新の要望にこたえ多年研究の結果，従来のキャッピングのあらゆるものにかわる高精度，超高速の供試体研磨仕上げ機で，各試験室等に必須品として絶賛を博しここに自信と喜びをもって御推奨する最新鋭機です。

特にJIS A1108に規定された圧縮強度試験の精度を得るために要求されています。

(1) 軸に垂直

(2) 仕上面　0.02 mm 以下

を得るための最適の機械です。

従来の様なキャッピングの〝むつかしさ〟を一挙に解決

キャッピングの〝熟練度〟は全く不要

ただ機械の上に置くだけで数分にして0.02 mm以下の平面度となる驚異的な高性能を有しています。

個人誤差皆無です。

ソイルテストの供試体のキャッピングも勿論出来ます。

特　長

1. 操作簡単(機械に供試体を取付取外しする作業全く不要，ただ供試体をおいて仕上げ剤をパラッとまくだけ)
2. キャッピングの熟練度は全く不要，研磨仕上げは数分間に出来ます。
3. 経済的です（仕上げ剤の経費は極く僅少）
4. 研磨面は手を労せず自然に0.02 mm以下の平面度を極めて確実に得る事が出来，従来の方法によるキャッピング面に得られない精度が容易に得られます。
5. 上下端面と円柱体との角度は90°に仕上ります。
6. 4.5.により供試体強度は当然正確に得られます。
7. 機械の注油全く無用（回転部はすべて密閉式ボールベアリング使用）
8. 乾式湿式両用に使用出来ます（掃除撤水に対し水密なる構造に設計されています）
9. 可搬移動式で堅牢
10. 使用範囲広し（研磨剤によりあらゆる物を美しく研磨する事が出来ます）

仕様の概要

1. 本体は電動機，減速機，伝達部を内蔵し，鋼板にて美麗に覆い，台上に研磨盤，揺動アーム，回転円筒を装置する。
2. 研磨盤上に供試体を置くのみにて供試体は一定位置にて円柱周面は回転円筒にそって揺動回転運動をし，揺動アームで左右に移動させつつ，回転運動中の研磨盤上を万遍なく研磨運動をする機構とする。
3. 大きさ及び速度（15 cmφ×30 cm の標準供試体用）

   供試体２ケ掛　630×　900×高サ 850 mm　三相（220 V）400 W(1/2HP) モーター付

   供試体３ケ掛　900 mmφ ×　高サ 850 mm　三相（220 V）400 W(1/2HP) モーター付

   供試体４ケ掛　850×1000×高サ 850 mm　三相（220 V）750 W(１HP) モーター付

   変速機　(5～50 r.p.m.)

   コード　５米　　ボタンスイッチ付
4. 運搬に便なる用，自在車および取手付
5. 取外し簡便なる水洗い掃除用特殊二ツ割受器を付しています。
6. 特別附属品　①特種研磨仕上げ剤　一袋

   ②湿式用の注水設備　一式

MARUI　株式会社 圓井製作所

本　　社　大阪市城東区蒲生町４ノ１０番地
電話　大阪（931）３５４１番（大代表）
(新)東京出張所　東京都港区芝田村町５ノ４番地(吉田ビル)
電話　東京（431）７　５　６　３　番

昭和三十七年五月二十八日第三種郵便物認可
昭和三十八年五月十五日印刷（毎月一回）
昭和三十八年五月二十日発行

木学会論文集第九十三号

定価百五十円